

## Measurement of the Dispersion of Thermal Ion-Acoustic Fluctuations in High-Temperature Laser Plasmas Using Multiple-Wavelength Thomson Scattering

D. H. Froula,\* P. Davis,<sup>†</sup> L. Divol, J. S. Ross,<sup>‡</sup> N. Meezan, D. Price, and S. H. Glenzer  
L-399, Lawrence Livermore National Laboratory, P.O. Box 808, Livermore, California 94551, USA

C. Rousseaux

CEA-DIF, Centre de Bruyères-le-Châtel, B.P. 12, 91680 Bruyères-le-Châtel, France

(Received 12 July 2005; published 3 November 2005)

The dispersion of ion-acoustic fluctuations has been measured using a novel technique that employs multiple color Thomson-scattering diagnostics to measure the frequency spectrum for two separate thermal ion-acoustic fluctuations with significantly different wave vectors. The plasma fluctuations are shown to become dispersive with increasing electron temperature. We demonstrate that this technique allows a time resolved local measurement of electron density and temperature in inertial confinement fusion plasmas.

DOI: 10.1103/PhysRevLett.95.195005

PACS numbers: 52.25.Os, 52.35.Fp, 52.50.Jm

Thermal density fluctuations in a plasma are the result of spontaneously generated electric and magnetic fields caused by the motion of charged particles. Probing these density fluctuations offers a unique way to measure equilibrium plasma conditions. Thomson-scattering measurements use an optical laser with a frequency ( $\omega_o$ ) and a wave number ( $k_o$ ) to elastically scatter from electron density fluctuations with a given wave vector ( $k$ ) [1,2]. Over the last 40 years, experiments have used Thomson scattering to extract fundamental plasma properties from the scattered frequency spectrum and it is now widely used in magnetic fusion and inertial confinement fusion research.

Thomson scattering is used as a diagnostic to probe the individual electrons in the noncollective regime, and resonant plasma fluctuations in the collective regime [3–6]. Resonant electron plasma fluctuations are observed when the light is scattered from electron density fluctuations with wavelengths larger than the Debye length ( $k_{epw}\lambda_{De} < 1$ ). Collective ion-acoustic features ( $k_a$ ) are observed when the probed electrons follow the motion of the ions ( $ZT_e/T_i > k_a^2\lambda_{De}^2$ ). In this regime the electrons move to screen the potential created by the ion fluctuations.

Ion-acoustic fluctuations provide the most intense features in the collective scattering spectrum and their frequency is commonly used to measure the electron temperature. Measuring electron plasma fluctuations [7–10] provides a measure of the electron density, but the relatively small scattered signal requires a high-power probe laser [7]. We present a new technique for simultaneously measuring local electron temperature and density that uses the ion-acoustic feature and, therefore, standard low power probe lasers can be employed ensuring that the plasma conditions are not perturbed.

The power spectrum for thermal density fluctuations in a plasma can be expressed using a theoretical form factor [11]:

$$S(k_a, \omega_a) = \frac{2\pi}{k_a} \left| 1 - \frac{\chi_e}{\epsilon} \right|^2 f_e\left(\frac{\omega_a}{k_a}\right) + \frac{2\pi Z}{k_a} \left| 1 - \frac{\chi_i}{\epsilon} \right|^2 f_i\left(\frac{\omega_a}{k_a}\right) \quad (1)$$

where  $\epsilon(\omega_a, k_a) = 1 + \chi_e + \chi_i$  is the plasma dielectric function. In a Maxwellian plasma, the phase velocity ( $v_\phi = \omega_a/k_a$ ) for low frequency ion-acoustic fluctuations is in the tail of the ion distribution function ( $f_i[(\omega_a/k_a) \gg v_\phi] \sim 0$ ) and near the peak of the electron distribution function ( $f_e[(\omega_a/k_a) \ll v_\phi] \sim 1$ ); therefore, Eq. (1) is dominated by the first term on the right hand side. The frequency of the resonant fluctuations will be near the point where  $\epsilon = 0$ . Previously, experiments have inferred the dispersion of ion-acoustic fluctuations by exciting small amplitude waves in low temperature plasmas ( $< 1$  eV,  $k_a\lambda_{De} < 1$ ) [12].

In this Letter, we present a novel measure of the dispersion of thermal ion-acoustic fluctuations in a dense high-temperature plasma for a variety of electron temperatures and densities ( $0.2 < k_a\lambda_{De} < 1.5$ ). In a high-temperature plasma, the frequency of ion-acoustic fluctuations is sensitive to both the local electron temperature and density. The use of Thomson-scattering diagnostics at multiple probe wavelengths allows us to measure the local frequency of the ion-acoustic fluctuations for two significantly different wave vectors. Because the dispersion of ion-acoustic waves is sensitive to Debye shielding, this technique is shown to be a powerful diagnostic of both the local electron density and local electron temperature with high temporal and spatial resolution which could be adapted for a variety of applications across the fields of plasma physics where other diagnostics have failed to provide accurate measurements.

This experiment used a four laser beam configuration at the recently upgraded Janus Long Pulse Facility at the Lawrence Livermore National Laboratory (Fig. 1). The

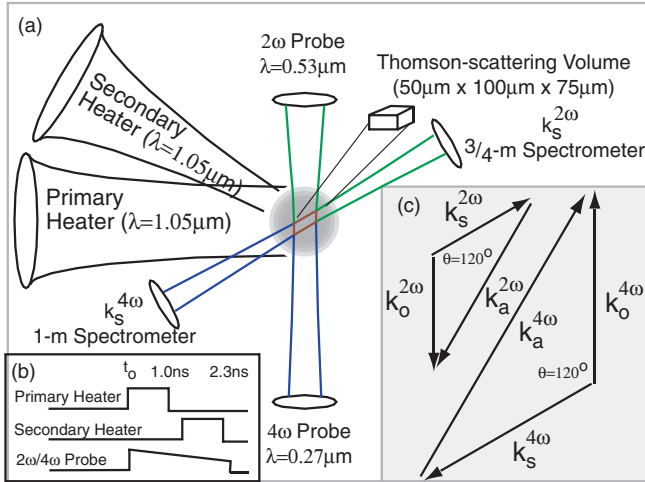


FIG. 1 (color). (a) The experimental setup is shown. (b) Beam timing. (c) A  $k$ -vector diagram shows the ion-acoustic waves,  $k_a \approx 4\pi/\lambda_{is} \sin\theta/2$ , that are probed.

nitrogen gas-jet plasmas were produced by two high-power ( $\lambda = 1054$  nm) laser beams. The neutral gas density was well-characterized using a Mach-Zender interferometer. The heater beams were pointed through the center of the 1 mm diameter gas jet, 1.5 mm from the jet exit. The primary heater beam used 450 J in a 1 ns laser pulse. The beam was focused to a 1.2 mm diameter focal spot at the target chamber center (TCC) through a phase zone plate using a  $f/6.7$  lens producing plasmas with a range of electron temperatures ( $100 \text{ eV} < T_e < 700 \text{ eV}$ ) and densities ( $10^{19} \text{ cm}^{-3} < n_e < 10^{20} \text{ cm}^{-3}$ ). The second heater beam used 100 J in 1 ns, 0.3 ns after the falling edge of the primary heater beam [Fig. 1(b)]. This beam was focused using a  $f/6.7$  lens with a continuous phase plate (CPP) to a 200  $\mu\text{m}$  diameter focal spot at the TCC.

Two 0.5 J Thomson-scattering probe lasers at two different wavelengths,  $\lambda_{2\omega} = 532$  nm and  $\lambda_{4\omega} = 266$  nm, were used to probe thermal ion-acoustic fluctuations with significantly different wave vectors. The  $2\omega$  and  $4\omega$  probe beams were focused using a  $f/5$  and  $f/10$  lens, respectively, to a diameter at the TCC of 75 microns. Through conservation of momentum, the ion-acoustic wave vector probed by each diagnostic ( $k_a$ ) is defined by the scattering geometry and the wavelength of the probe laser [Fig. 1(c)].

Two  $f/5$  collection lenses collimated light scattered from a single Thomson-scattering volume in the plasma. The scattered light was then focused onto the slit of a 3/4 meter (for  $2\omega$ ) and a 1 meter (for  $4\omega$ ) imaging spectrometers using two  $f/10$  focusing lenses. The optical configurations provided a magnification of two. The spectrometers were coupled to Hamamatsu streak cameras. The linear dispersion for the  $2\omega$  and  $4\omega$  Thomson-scattering diagnostics were 0.0047 nm/pixel and 0.0012 nm/pixel respectively. The instrument resolution was  $\text{FWHM}_{2\omega} = 12$  pixels (0.056 nm) and  $\text{FWHM}_{4\omega} = 18$  pixels (0.021 nm) defined by 100  $\mu\text{m}$  slits on the entrance of the spectrometers.

The Thomson-scattering volume was defined in space using a small glass ball that was suspended over the center of the gas jet. All beams were aligned to the ball at the TCC. The glass ball was backlit and imaged through the  $2\omega$  and  $4\omega$  Thomson-scattering diagnostics. The ball was viewed through the streak camera in focus mode and both the spectrometer and the streak camera slits were closed around the center of the ball. This defined a  $2\omega$  and a  $4\omega$  Thomson-scattering volume ( $50 \mu\text{m} \times 100 \mu\text{m} \times \sim 75 \mu\text{m}$ ) located at the TCC. While the absolute radial position between the gas jet and the Thomson-scattering volumes was a few hundred microns, the relative position between data points was better than 50  $\mu\text{m}$ .

Figure 2 shows our measurements of the dispersion of ion-acoustic fluctuations for a range of densities by comparing the phase velocities of the two independently measured ion-acoustic wave vectors ( $\Delta \propto v_{\phi}^{2\omega} - v_{\phi}^{4\omega}$ ). Each set of points corresponds to the temporal evolution in the electron temperature for a given density on a single shot. In order to clearly observe the effects of the dispersion on the ion-acoustic fluctuations, the  $2\omega$  Thomson-scattering results were normalized by the ratio in wave vectors ( $k_{4\omega}/k_{2\omega} = 2$ ); therefore, the difference between the normalized  $2\omega$  wavelength separation and the  $4\omega$  wavelength separation [ $\Delta = (\Delta\lambda_{2\omega}/2) - \Delta\lambda_{4\omega}$ ] is zero for a nondispersive plasma. The wavelength separation between the spectral features for each Thomson-scattering diagnostic ( $\Delta\lambda_{is}$ ), at various times (every 200 ps), was determined using independent Gaussian fits to both sides of the Thomson-scattering spectra.

Figure 2(b) shows good agreement between the measured and calculated ion-acoustic frequencies over a large range of densities and temperatures. These results confirm

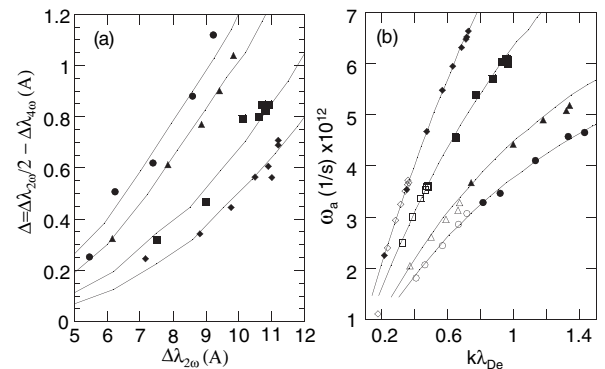


FIG. 2. (a) As the electron temperature increases (increasing  $\Delta\lambda_{2\omega}$ ) or the electron density decreases (each curve represents a single density), the plasma becomes more dispersive; the normalized wavelength difference ( $\Delta$ ) in a nondispersive plasma would follow the  $x$  axis ( $\Delta = 0$ ). (b) The open (closed) symbols are the measured ion-acoustic frequencies from the  $2\omega$  ( $4\omega$ ) diagnostics. The solid lines are calculated using Eq. (1) for the densities experimentally measured using Thomson scattering (diamonds)  $n_e(r=0 \mu\text{m}) = 1.2 \times 10^{20} \text{ cm}^{-3}$ , (squares)  $n_e(r=350 \mu\text{m}) = 7.0 \times 10^{19} \text{ cm}^{-3}$ , (triangles)  $n_e(r=550 \mu\text{m}) = 3.5 \times 10^{19} \text{ cm}^{-3}$ , (circles)  $n_e(r=700 \mu\text{m}) = 2.5 \times 10^{19} \text{ cm}^{-3}$ .

the dispersion of ion-acoustic fluctuations; when the wavelength of the fluctuation is larger than the electron Debye length ( $\lambda_{De} = \sqrt{\epsilon_0 T_e / n_e e^2}$ ), the plasma is nondispersive. In this limit, the phase velocity is equal to the group velocity ( $\omega_a/k_a = d\omega_a/dk_a = c_s$ ). As the electron temperature increases for a given density, the electron screening is less effective and the phase velocity of the ion-acoustic fluctuations are dependent on the wave-number ( $d\omega_a/dk_a < c_s$ ).

The measured frequencies for the ion-acoustic fluctuations shown in Fig. 2 were determined directly by the wavelength separation in the spectral features measured by Thomson scattering,  $\omega_a = (\pi c / \lambda_{ts}^2) \Delta \lambda_{ts}$ . The Debye length for each point was measured by simultaneously fitting the form factor [Eq. (1)] to the  $2\omega$  and  $4\omega$  spectra. This can be illustrated by solving for the ion-acoustic phase velocity in the fluid limit,

$$\frac{\omega_a}{k_a} = \sqrt{\frac{ZT_e}{M(1 + k_a^2 \lambda_{De}^2)} + \frac{3T_i}{M}}. \quad (2)$$

Concurrently measuring two independent ion-acoustic frequencies with significantly different wave vectors allows a unique solution to Eq. (2) that provides a direct measure of the electron temperature and density.

Figure 3 shows a set of fits for a Thomson-scattering volume located at  $r = 550 \mu\text{m}$ . The constant density curves in Fig. 2 were calculated by the theoretical form factor [Eq. (1)] using the densities measured with Thomson scattering. For these fits an ion temperature ( $T_i/T_e = 0.3$ ) and average charge state ( $Z = 7$ ) was assumed; the main results of this paper are not sensitive to the ion temperature as long as  $T_i \ll T_e$ . Hydrodynamic simulations discussed below show the plasma is fully ionized within the first 100 ps of the experiment.

Using the results from Fig. 2, the density profile in the gas jet was measured and shows good agreement to the independent interferometer measurements (Fig. 4). For each shot, the electron density was determined at the time of peak temperature where the system is most sensitive to electron density. The relative error in the position of the density measurement is shown by the horizontal error bars; the absolute radial position of the data set was moved by  $200 \mu\text{m}$  which is within the positioning error previously discussed. The density profiles are shown to vary by less than 20% over the time of the experiment using a hydrodynamic simulation performed with the code HYDRA (Fig. 4) [13]. The HYDRA simulations used the experimental laser parameters and the 3-dimensional neutral gas density profile measured using interferometry as initial conditions.

The error bars shown for the measured density data in Fig. 4 were determined by the error in the measurement from both ion-acoustic frequencies. Figure 5 shows a series of calculations where the parameter space around the measured electron temperature and density was determined using the actual measurement uncertainties for

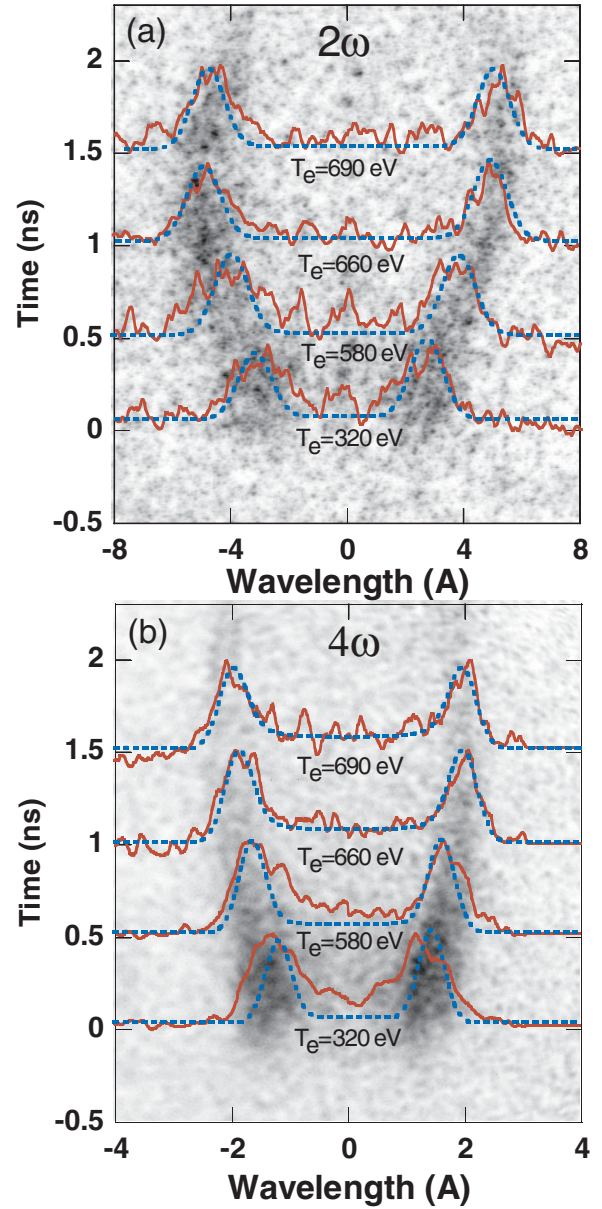


FIG. 3 (color). Thomson-scattering data from the same scattering volume in the gas-jet plasma shows the dispersive nature of the plasma; as the plasma temperature increases, the  $2\omega$  spectral features increase faster than the  $4\omega$  features. The two detectors measured the local ( $r = 550 \mu\text{m}$ ) electron temperature as a function of time and the time average local density ( $n_e = 3.2 \times 10^{19} \text{ cm}^{-3}$ ). The theoretical form factor is fit for each time (dashed, blue line).

each Thomson-scattering diagnostic ( $\delta\lambda_{4\omega} = 0.0014 \text{ nm}$  and  $\delta\lambda_{2\omega} = 0.005 \text{ nm}$ ). When the electron temperature is low, the wavelength separation is small. If  $k_a \lambda_{De}$  is also low, the diagnostic is insensitive to density and the error in the density results are dominated by the error in the measurement of the ion-acoustic peaks (bottom right area in Fig. 5).

This technique is well suited for large laser facilities where other diagnostics have not been successful in mea-

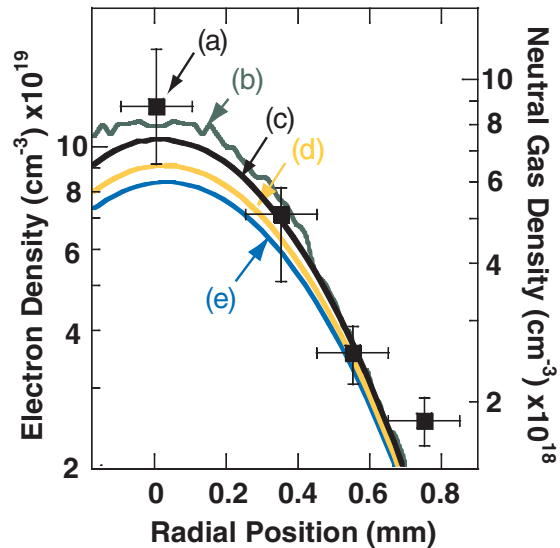


FIG. 4 (color). (a) Two Thomson-scattering diagnostics were used to measure the electron density profile of the plasma (squares). (b) The 3D neutral density profile (green curve) for the gas jet was measured using interferometry 1.5 mm above the gas jet (right axis). Hydrodynamic simulations used the initial measured 3-D profile to calculate the electron density; (c)  $t = 0.25$  ns, (d)  $t = 0.5$  ns, (e)  $t = 1.0$  ns.

asuring local electron plasma density and temperature. Two ion-acoustic frequencies can be measured by either using two probe wavelengths or a single probe laser with two significantly different scattering angles. A small angle diagnostic ( $k_a^1$ ) can be chosen to provide a good measure of the electron temperature with a small dependence on the density ( $k_a^1 \lambda_{De} < 1$ ) while a large angle diagnostic ( $k_a^2$ ) would provide a good measure of the electron density ( $k_a^2 \lambda_{De} > 1$ ). There is a limitation for large angles (for a given probe wavelength) given by the constraint of remaining in the collective Thomson-scattering regime ( $ZT_e/T_i \gg k_a^2 \lambda_{De}^2$ ) while there is a practical limit for small angles given by the instruments ability to resolve the spectral peaks (i.e., the wavelength separation scales with the angle).

For a typical inertial confinement fusion plasma ( $T_e = 5$  keV,  $n_e = 5 \times 10^{20}$  cm $^{-3}$ ) the optimal scattering angles for the two collection optics are  $40^\circ < \theta_{k2} < 80^\circ$  ( $0.4 < k_2 \lambda_{De} < 0.7$ ) and  $\theta_{k1} > 140^\circ$  ( $k_1 \lambda_{De} > 0.9$ ); using these scattering angles, a single  $4\omega$  probe laser, and typical instrument resolutions, the local density could be measured to better than 25% with an electron temperature measurement to within 10%.

In summary, we have shown that the phase velocity of ion-acoustic fluctuations is dependent on their frequency; this measure of the dispersion of ion-acoustic fluctuations is of great importance for the understanding of ion-acoustic fluctuations in dense high-temperature plasmas. Furthermore, we have demonstrated a novel technique for measuring the electron density and temperature which is in

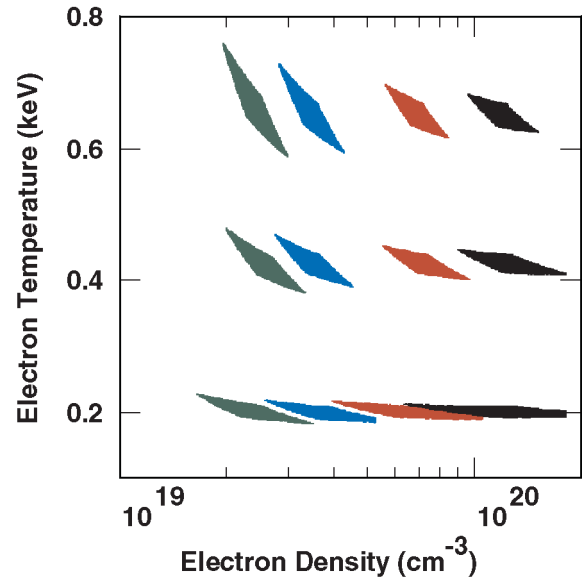


FIG. 5 (color). Each parameter space was calculated for the measured electron densities and temperatures using the actual measurement errors for each Thomson-scattering diagnostic. The error bars in Fig. 4 were determined using the extreme values in the calculated parameter space for each measured density at the peak electron temperature.

good agreement with independent interferometry measurements and hydrodynamic simulations.

We would like to acknowledge the efforts of the Janus Laser Crew. We thank S. Dixit, M. Rushford, C. Hoaglan, and M. Aasen for the design and a fabrication of the CPP. Furthermore, we thank R. Griffith for the streak camera support. This work was performed under the auspices of the U.S. Department of Energy by the Lawrence Livermore National Laboratory under Contract No. W-7405-ENG-48.

\*Electronic address: froula1@llnl.gov

†Also at Engineering Department, University of British Columbia.

‡Also at Department of Applied Science, University of California at Davis.

- [1] H.-J. Kunze *et al.*, Phys. Lett. **11**, 42 (1964)
- [2] A. A. Offenberger *et al.*, Phys. Rev. Lett. **71**, 3983 (1993).
- [3] B. S. Bauer *et al.*, Phys. Rev. Lett. **74**, 3604 (1995).
- [4] H. A. Baldis *et al.*, Can. J. Phys. **64**, 961 (1986).
- [5] P. E. Young, Phys. Rev. Lett. **73**, 1939 (1994).
- [6] D. H. Froula *et al.*, Phys. Rev. Lett. **88**, 105003 (2002).
- [7] S. H. Glenzer *et al.*, Phys. Rev. Lett. **82**, 97 (1999).
- [8] E. Fourkal *et al.*, Phys. Plasmas **8**, 550 (2001).
- [9] S. C. Snyder *et al.*, Phys. Rev. E **50**, 519 (1994).
- [10] G. Gregori *et al.*, Phys. Rev. E **59**, 2286 (1999).
- [11] J. A. Fejer, Can. J. Phys. **38**, 1114 (1960).
- [12] H. Tanaka *et al.*, Phys. Rev. Lett. **16**, 1079 (1966).
- [13] M. Marinak *et al.*, Phys. Plasmas **5**, 1125 (1998).